21st Australasian Fluid Mechanics Conference
Adelaide, Australia
10-13 December 2018

Large Eddy Simulation of Flow Over Streamwise Heterogeneous Canopies: Quadrant Analysis

D. Sutherland[1,3,4], J. Philip[2], A. Ooi[2] and K. A. M. Moinuddin[3,4]

[1]School of Physical, Environmental, and Mathematical Sciences
University of New South Wales, Canberra, Australian Capital Territory 2610, Australia

[2]Department of Mechanical Engineering
University of Melbourne, Melbourne, Victoria 3010, Australia

[3]Institute for Sustainable Industries and Livable Cities
Victoria University, Melbourne, Victoria 8001, Australia

[4]Bushfire and Natural Hazards Cooperative Research Centre
East Melbourne, Victoria 3002, Australia

Abstract

Large eddy simulations of flow over heterogeneous forest canopies are performed. Each simulated forest consists of equal-sized strip canopies which alternate in the streamwise direction between sparse and dense leaf area density. Quadrant analysis is then used to investigate the eddy fluxes near the top of the forest with an eye towards developing a parameterisation of particle motion through the forest. The quadrant analysis demonstrates that the sweep-ejection cycle is modified by the canopy heterogeneities. The greatest modifications occur with the largest difference in leaf area densities. Ejections appear to be enhanced over canopy heterogeneities of intermediate length. Forests with large length-scale heterogeneities and forests with short length-scale heterogeneities are qualitatively similar to uniform canopies.

Introduction

The characteristics of the turbulent flow within and immediately above tree canopies has implications for simulating ember transport in wildfires. Embers are often modelled as Lagrangian particles and modern Lagrangian particle transport models use quadrant analysis of the sweep-ejection cycle to parameterise the forces due to turbulent fluctuations which act upon the particle [9]. The probability distribution of turbulent fluctuations $P(u',w')$ in the streamwise and vertical directions are classified into outward interactions, ejections, inward interactions, and sweeps. The aim of this study is to examine the effect of canopy heterogeneity on the sweep-ejection cycle with an eye to developing a parameterisation of particle motion. The shear layer immediately above the canopy and the sub-canopy flow are strongly influenced by the distribution of plant material, the leaf area density (LAD), within the canopy. The LAD is typically heterogeneous and varies across different types of forest. These heterogeneities affect the above- and sub-canopy flow particularly at boundaries between different forests. Pressure-gradient driven large eddy simulations (LES) are conducted in a fixed-size periodic channel domain with an idealised forest canopy, constructed of stripes with alternating sparse and dense forests, which is analogous to previous simulations conducted over heterogeneous rough surfaces [3] . The forest canopy is modelled as a region of aerodynamic drag, where the drag force varies between the different stripes [12]. Analogous to Bou Zeid et al. [3], set of 15 simulations are conducted over a three parameter space: $(N_c, \alpha_s, \alpha_d)$, the total number of canopies of both type $N_c = 1,2,4,8,16$ and $\alpha_{s,d} = 0.05, 0.2, 0.4$ (α_s for the sparse canopy and α_d for the dense canopy), see figure 1 for a four-canopy domain case. Firstly we will provide a qualitative overview of the flow by discussing a prototypical four-canopy case. Then we compare the quadrants of $P(u',w')$ at the canopy tops for all heterogeneous canopy cases.

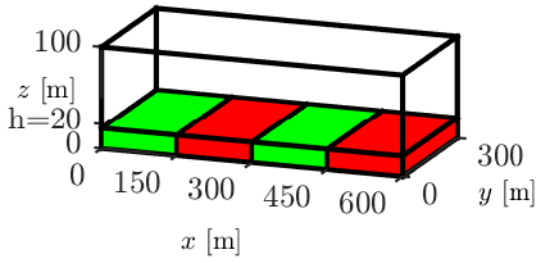

Figure 1: Example simulation domain $N_c = 4$; sparse canopies are green and dense canopies are red.

Numerical setup

In these LES the equations describing conservation of mass and momentum in a fluid (the continuity and Naiver-Stokes equations respectively) are spatially filtered retaining the dynamically important large-scale structures of the flow. In FDS the filtering operation is implicit at the grid scale. The effect of the turbulent smaller scales eddies on the resolved large scale eddies is then modelled.

$$\frac{\partial \overline{\rho}\tilde{u}_i}{\partial t} + \frac{\partial \overline{\rho}\tilde{u}_i\tilde{u}_j}{\partial x_j} = -\frac{\partial \overline{p}}{\partial x_i} - \frac{\partial \tau_{ij}}{\partial x_j} + \sum_k f_{D,i,j,k} \,. \qquad (1)$$

τ represents the viscous and sub-grid scale turbulence stresses,

$$\tau_{i,j} = -2(\mu+\mu_t)\left(\frac{1}{2}\left(\frac{\partial u_i}{\partial x_j} + \frac{\partial u_j}{\partial x_i} - \frac{1}{3}\frac{\partial u_i}{\partial x_i}\delta_{ij}\right)\right) \qquad (2)$$

The eddy viscosity, μ_t, represents the diffusion from the sub-grid scale turbulence. The subgrid-scale stresses are modelled using the standard Smagorinsky model with Smagorinsky constant $C = 0.1$.

The canopy is modelled as an aerodynamic drag term of the form

$$F_{D,i,j,k}(z) = \frac{\rho}{2} c_D \chi_k(x,z,h) u_i(u_j u_j),. \qquad (3)$$

We fix the value to be $c_D = 0.25$ roughly consistent with the measurements of Amiro [1] and the study of Cassiani et al. [5].

The function $\chi_k(x,z,h)$, defines the spatial location of the k^{th} canopy. The canopy is sharply defined region, that is

$$\chi_k(x,z,h) = \begin{cases} \alpha_k & x_{0,k} < x < x_{1,k}\,, \quad y_{0,k} < y < y_{1,k}\,, \\ & 0 < z < h\,, \\ 0 & \text{otherwise}\,. \end{cases}$$

The leaf area density of the canopy α_k alternates between the sparse and dense values shown in table 1. A better representation of a real forest is to allow a vertical profile of leaf area density, rather than the constant profile chosen here. However, in the interest of controlled numerical experiments we idealise the canopy to have a uniform profile. Furthermore, to see the most obvious effects the uniform profiles are chosen to match a very sparse canopy, such as an open regrowth eucalyptus forest [10], and a very dense canopy such as a spruce forest [1]. The fifteen simulated cases are tabulated in table 1. The size of the exterior domain is chosen so that the largest relevant structures are captured. The channel sizes ($600 \times 300 \times 100$ m) are chosen to follow the proportions set out by Moser et al. [11]. The channel height is dictated by the canopy height. Bou Zeid et al. [4] recommend the channel height be at least four times larger the canopy height to avoid any artificial interaction between the top boundary and the canopy. The resolution is selected to be 5 m in both the $x-$ and $y-$directions and stretched between 0.5 to 4 m in the $z-$direction. $120 \times 60 \times 50$ discretisation points are used. The domain is periodic in the $x-$ and $y-$directions with no-slip and stress-free boundary conditions imposed at $z = 0$ and $z = 100$ m respectively. The driving pressure gradient is $\partial p/\partial x = 5 \times 10^{-3}$ Pa/m. The velocity fields are initialised from a constant velocity, with some random perturbations to ensure tripping to turbulence. The spin-up time was approximately 3600 s the simulation time was approximately 7200 s and statistics were sampled every 2 s. The data was sampled after the time series of turbulent kinetic energy had reached a steady state.

Table 1: Cases simulated

Case	N_c	L_c (m)	α (m^{-1})	α_d/α_s
C1L05	1	600	0.05	-
C1L2	1	600	0.2	-
C1L4	1	600	0.4	-
C2L05L2	2	300	0.05, 0.2	4
C4L05L2	4	150	0.05, 0.2	4
C8L05L2	8	75	0.05, 0.2	4
C16L05L2	16	37.5	0.05, 0.2	4
C2L05L4	2	300	0.05, 0.4	8
C4L05L4	4	150	0.05, 0.4	8
C8L05L4	8	75	0.05, 0.4	8
C16L05L4	16	37.5	0.05, 0.4	8
C2L2L4	2	300	0.2, 0.4	2
C4L2L4	4	150	0.2, 0.4	2
C8L2L4	8	75	0.2, 0.4	2
C16L2L4	16	37.5	0.2, 0.4	2

Results and Discussion

The case C4L05L4 is firstly examined to provide a qualitative understanding of the flow. Contours of non dimensionalised $u-$velocity, $w-$velocity, and $u'w'-$stress are shown in figure 2(a-c).

The velocities, stresses, and TKE are non dimensionalised used using the canopy top friction velocity averaged across all of the canopies. That is,

$$u_* = \langle \frac{\tau}{\rho} \rangle_x = \langle \nu \frac{\partial \langle u \rangle_{t,y}}{\partial z} - \langle u'w' \rangle_{t,y} \rangle_x\,, \tag{4}$$

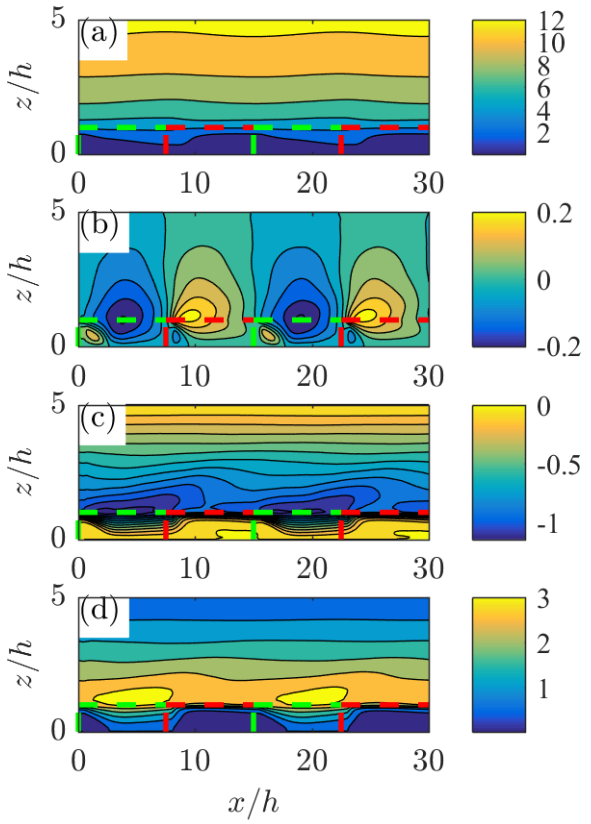

Figure 2: Contours of (a) non dimensional $y,t-$averaged $u-$velocity (b) non dimensional $y,t-$averaged $w-$velocity showing the strong up- (yellow) and down-drafts (blue) above and within the canopies. (c) Reynolds stress $u'w'$. (d) turbulent kinetic energy showing enhanced turbulence over the sparse canopies. The canopy stripes are shown as dotted outlines.

where τ is the total shear stress at the top of the canopy. Angled brackets denoted quantities averaged with respect to the subscripts. For example $\langle u \rangle_t$ is the time average of the $u-$velocity. Large-scale periodic variation in velocities and shear stress are observed with a length-scale equal to L_c. As the flow transitions from a sparse canopy to a dense canopy the mean $u-$velocity decreases and, by continuity, the mean $w-$velocity increases above the canopy leading to an updraft at the upstream edge of a dense canopy. Belcher et al. [2] refer to similar regions at the upstream edge of a single isolated canopy as *impact* regions. Similarly, at the transition from a dense canopy to a sparse canopy there is a downdraft associated with a streamwise acceleration in the sparse canopy. Enhanced turbulent fluctuations are often observed at the upstream edge of real forest canopies; such regions are referred to as enhanced gust zones [6]. The contours of $u'w'-$stress show enhanced shear stress in and above the sparse canopies. Enhanced turbulence in and above the sparse canopies are confirmed by the contours of $TKE = (u' + v' + w')/2$ shown in figure 2(d). There are prominent local maxima of TKE above the sparse canopies and the TKE in the sparse canopies is clearly greater than the TKE within the dense canopies.

Velocity-couplets visible in the contours of vertical velocity (eg. figure 2(b) at $(x,z) = (9, 0.5)$) suggest the emergence of mean recirculation regions within the sparse canopies near the dense-sparse boundaries. Indeed for large α_d/α_s recirculation regions, similar to those observed by Cassiani et al. [5] at the

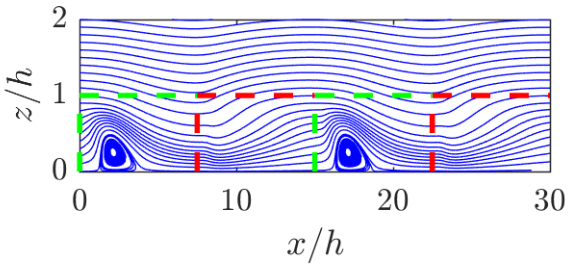

Figure 3: The streamlines through the heterogeneous canopies. The canopy stripes are shown as dotted outlines. Recirculation regions downstream of a dense-to-sparse transition are clearly visible at $x/h \approx 2$ and $x/h \approx 17$

downstream boundary of a single isolated canopy, form in the lower parts of the sparse canopies. Weaker recirculation regions are also observed for the $\alpha_d/\alpha_d = 8$, $N_c = 2, 8$, and 16 cases. However, recirculation regions are not observed for the other values of α_d/α_s. Proto-recirculation regions, they are regions where the streamlines are noticeably curved down stream of the dense-sparse interfaces, do exist for all other cases. The curved streamlines suggest that the emergence of a persistent vortex has not yet occurred but the parameters are near the critical values. Investigating the emergence of recirculations is of future interest. The recirculation region C4L05L4 are visualised by plotting the streamlines of the mean flow in figure 3.

The quadrant analysis of this flow is motivated by the stochastic particle transport model proposed by Jin et al. [9]. [9] Jin et al. model particle motion as a discrete random walk where the particle is subjected to forces from the mean fluid velocities and the fluctuating fluid velocities. In their model the mean fluid velocities are obtained from RANS models with a $k-\varepsilon$ model of turbulence. The interaction of the particles with turbulent eddies is modelled using a Markov chain process. The parameters of the Markov chain process are obtained using the probability density function (PDF) of the streamwise fluctuations u' and vertical w', that is, $P(u',w')$. The structure of Reynolds stress are usually classified into four quadrants based on the signs the instantaneous fluctuations u' and w'. The first quadrant Q1 interactions, $u' > 0$, $w' > 0$, are called outward interactions; Q2 interactions, $u' < 0$, $w' > 0$, are called ejections; Q3, $u' < 0$, $w' < 0$, are called inward interactions, and Q4 are $u' > 0$ $w' < 0$ called sweeps [13]. The sweep-ejection cycle is well-known to be modified by plant canopies; the major contribution to eddy fluxes above a tree canopy is from sweeps rather than ejections [7]. Given the up- and down-drafts (enhanced positive and negative $\overline{w}-$velocity) over the dense and sparse canopies respectively, the sweep-ejection cycle should be modified by the canopy heterogeneities. In particular, we may expect increased ejection motions at the sparse-dense interfaces and enhanced sweeping motions over the dense canopies. The parameter space considered here is large: N_c and α_d/α_s both vary, and the sweep-ejection cycle is likely different above the sparse canopies, the dense canopies, and the interfaces between the canopies. To gain a useful understanding of the sweep-ejection cycle above the heterogeneous canopies we compare $P(u',w')$ for $N_c = 2, 4, 8$, and 16 canopies for fixed α_d/α_s. The $P(u',w')$ distributions are computed at one grid cell above the canopy top. The quadrants are shown in figure 4(a) for $\alpha_d/\alpha_s = 8$, (b) for $\alpha_d/\alpha_s = 4$, and (c) for $\alpha_d/\alpha_s = 2$. The two single uniform canopy reference cases are also shown in each contour plot.

Several general trends are inferable from figure 4. Firstly, as expected, sweeping motions strongly dominate the eddy fluxes;

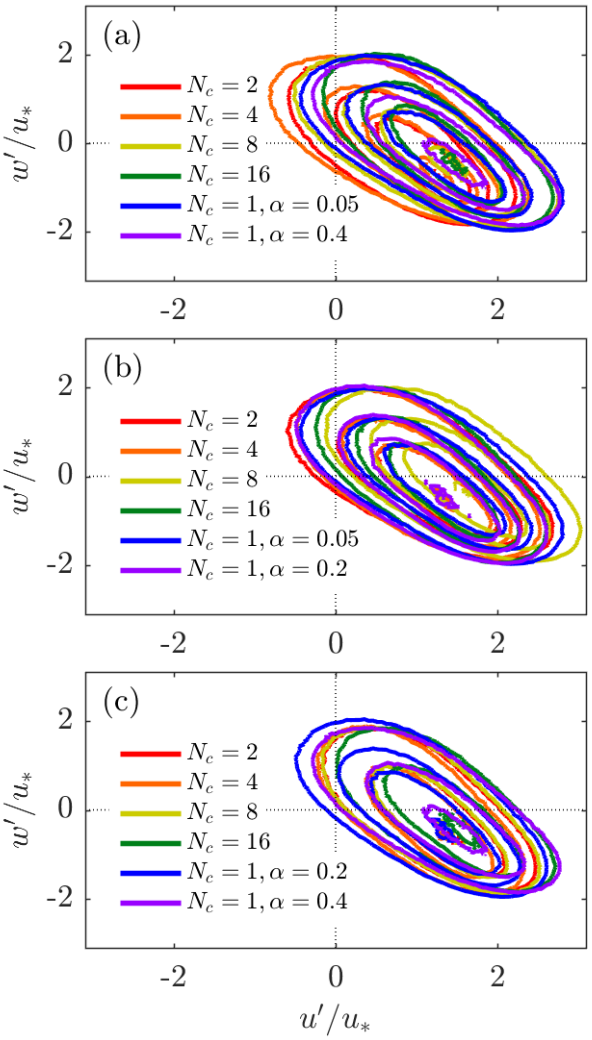

Figure 4: The quadrants of $P(u',w')$ for (a) for $\alpha_d/\alpha_s = 8$, (b) for $\alpha_d/\alpha_s = 4$, and (c) for $\alpha_d/\alpha_s = 2$. Contours levels are $[0.1, 0.3, 0.5, 0.7] \times 10^{-3}$

consistent with the prior findings discussed in Finnigan [7]. The $\alpha_d/\alpha_s = 8$ case exhibits the most variation in the quadrants; this result is unsurprising. The largest changes in the streamwise and vertical velocities will occur with the largest differences in applied drag forces and hence with the biggest difference between the sparse and dense canopy leaf area densities. The distribution tends to be narrower, that is the distribution has less variance, as α_d/α_s decreases. The $N_c = 2$ and $N_c = 16$ cases tend to have distributions similar to the reference single uniform canopies, whereas the distributions of the $N_c = 4$ and $N_c = 8$ cases tend to be shifted away from the reference uniform canopy cases. It is hypothesised that the $N_c = 2$ and $N_c = 16$ canopy cases tend mimic the single uniform canopies more consistently than the $N_c = 4$ and $N_c = 8$ cases. The $N_c = 2$ cases have long canopy lengths which allow the flow to adjust the different canopy. The $N_c = 16$ case changes undergoes rapid changes in leaf area density and therefore may appear similar to a uniform canopy, albeit with some intermediate leaf area density. The quadrants suggest that for the $N_c = 2$, $\alpha_d/\alpha_s = 2$ and $\alpha_d/\alpha_s = 4$ cases the eddy fluxes are similar to the uniform reference canopies. For the $\alpha_d/\alpha_s = 8$ case the ejection motions are slightly enhanced. For $N_c = 16$ and $\alpha_d/\alpha_s = 8$ values the distri-

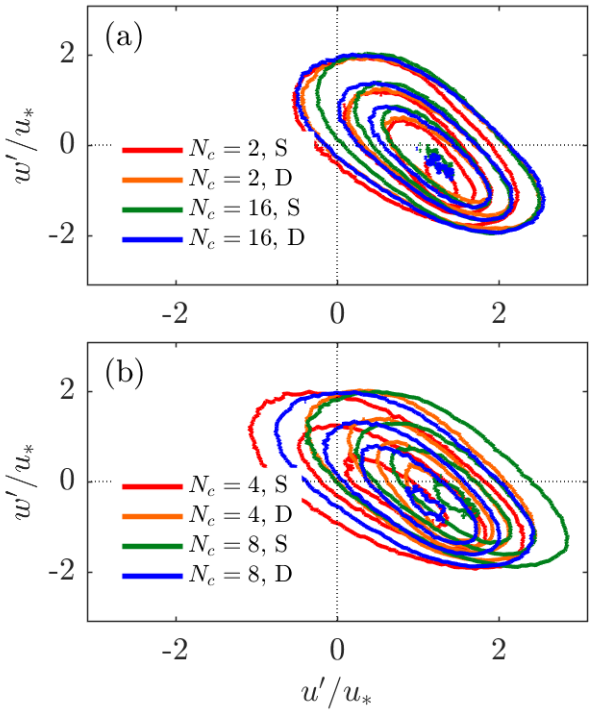

Figure 5: $P(u',w')$ for $\alpha_d/\alpha_s = 8$ computed conditionally over the (S) sparse and (D) dense canopies. Contour levels are as before.

bution is qualitatively similar to the distribution of the uniform reference cases. In the $\alpha_d/\alpha_s = 2$ and 4 $N_c = 16$ cases the distribution tends to have smaller spread than the uniform reference canopies. The two contours of particular interest are the $N_c = 4$ and $\alpha_d/\alpha_s = 8$ case and the $N_c = 8$ and $\alpha_d/\alpha_s = 4$ case. For the $N_c = 4$ and $\alpha_d/\alpha_s = 8$ case the ejections are considerably enhanced, however, this is the tail of the distribution, the peak location remains in the third quadrant. The $\alpha_d/\alpha_s = 4$ and the $N_c = 8$ case appears to have shifted to increased positive u'. In this case ejections are diminished relative to the $N_c = 2,4$, and 16 cases as well as the uniform reference cases and the motion is dominated by outward interactions and sweeps. To further investigate the role of the canopy density interfaces, the distributions of $P(u',w')$ for $\alpha_d/\alpha_s = 8$, that is the case where the most variation in the distribution is expected, are computed over the sparse canopies and the dense canopies separately and are shown in figure 5. The sparse and dense $P(u',w')$ for $N_c = 2$ and $N_c = 16$ (figure 5(a)) are qualitatively similar and exhibit no significant trends. However, $P(u',w')$ for $N_c = 4$ and $N_c = 8$ (figure 5(b)) exhibit considerable variation, although without a systematic trend. The $N_c = 4$ sparse and $N_c = 8$ dense canopies exhibit enhanced ejection motions relative to the $N_c = 4$ dense and $N_c = 8$ sparse canopies.

Conclusions

Simulations of flow over forests with strips of alternating leaf area density were conducted with the intention revealing the effect of the heterogeneities on the eddy fluxes at the canopy top. The eddy fluxes at the canopy top were characterised by the quadrants of $P(u',w')$. The quadrants are only significantly modified if the ratio between the leaf area densities α_d/α_s is large enough. The results also reveal that if the canopy heterogeneities are relatively large, or relatively small, the heterogeneous canopy has $P(u',w')$ similar to a uniform forest. There is some intermediate canopy length scale where the ejection eddy fluxes above the canopies are enhanced. Further work is required to adapt the particle model of Jin et al. [9] for flow through plant canopies.

Acknowledgements

The authors wish to acknowledge the a high performance computing facilities at the University of Melbourne. This work was funded by the BNHCRC.

References

[1] Amiro, B.D. Comparison of turbulence statistics within three boreal forest canopies. *Boundary-Layer Meteorology*, 51(1-2):99–121, 1990.

[2] Belcher, S.E., Jerram, N., Hunt, J.C.R. Adjustment of a turbulent boundary layer to a canopy of roughness elements. *Journal of Fluid Mechanics*, 488:369–398, 2003.

[3] Bou-Zeid, E., Meneveau, C.,and Parlange, M.B. Large-eddy simulation of neutral atmospheric boundary layer flow over heterogeneous surfaces: Blending height and effective surface roughness. *Water Resources Research*, 40 (2), 2004.

[4] Bou-Zeid, E., Overney, J., Rogers, B.D., and Parlange, M.B., The effects of building representation and clustering in large-eddy simulations of flows in urban canopies. *Boundary-Layer Meteorology*, 132(3):415–436, 2009.

[5] Cassiani, M., Katul G.G., and Albertson, J.D., The effects of canopy leaf area index on airflow across forest edges: large-eddy simulation and analytical results. *Boundary-Layer Meteorology*, 126(3):433–460, 2008.

[6] Dupont, S., Bonnefond, J-M., Irvine, M.R., Lamaud, E., and Brunet, Y. Long-distance edge effects in a pine forest a deep and sparse trunk space: in situ and numerical experiments. *Agricultural and forest meteorology*, 151: 328–344, 2011.

[7] Finnigan, J. Turbulence in plant canopies. *Annual Review of Fluid Mechanics*, 32(1):519–571, 2000.

[8] Inoue, E. On the turbulent structure of airflow within crop canopies. *Journal of the Meteorological Society of Japan. Ser. II*, 41(6):317–326, 1963.

[9] Jin, C., Potts, I., and Reeks, M.W. A simple stochastic quadrant model for the transport and deposition of particles in turbulent boundary layers. *Physics of Fluids*, 27 (5):053305, 2015.

[10] Moon K., Duff, T.J., and Tolhurst, K. G. Sub-canopy forest winds: understanding wind profiles for fire behaviour simulation. *Fire Safety Journal*, 2016. In press.

[11] Moser, R.D., Kim, J., and Mansour, N.N., Direct numerical simulation of turbulent channel flow up to re τ= 590. *Physics of fluids*, 11(4):943–945, 1999.

[12] Mueller, E., Mell, W., and Simeoni, A. Large eddy simulation of forest canopy flow for wildland fire modeling. *Canadian Journal of Forest Research*, 44(12):1534–1544, 2014.

[13] Wallace. J.M. Quadrant analysis in turbulence research: history and evolution. *Annual Review of Fluid Mechanics*, 48:131–158, 2016.